Segmentation of Lung Fields by Game Theory and Dynamic Programming

Bulat Ibragimov, Tomaž Vrtovec, Boštjan Likar and Franjo Pernuš

University of Ljubljana, Faculty of Electrical Engineering, Slovenia
{bulat.ibragimov, tomaz.vrtovec, bostjan.likar, franjo.pernus}@fe.uni-lj.si

Abstract. Segmentation of medical images is widely used to delineate anatomical and other structures, with the aim to diagnose various disorders, locate pathology, create models and statistical atlases, quantify structural properties, etc. In this paper we propose a supervised algorithm for lung fields segmentation, which is based on game theory and dynamic programming. To define a game, a set of "players", a set of "strategies" and a set of "incomes" are required. For segmentation purposes these sets correspond to distinctive anatomical points (i.e. landmarks), image features consisting of intensities and geometrical relationships between landmarks and the matrix of incomes depending on the image features. The solution of the game named arbitration scheme gives the best positions of landmarks. Boundary segments between adjacent landmarks are then detected by dynamic programming that is based on the Bellman principle of optimality. The results of the lung fields segmentation algorithm are evaluated by the overlap measure and compared to segmentation methods based on pixel classification, active shape and active appearance models.

Keywords: Segmentation, multi-criteria optimization, game theory, dynamic programming, lung fields

1 Introduction

Segmentation of medical images is widely used to delineate anatomical and other structures, with the aim to diagnose various disorders, locate pathology, create models and statistical atlases, quantify structural properties, etc. Segmentation of bony structures is usually accomplished by intensity based methods such as thresholding, region growing and clustering [1, 2]. However, precise segmentation by these methods often fails, because of the large biological variability of normal and pathological anatomical structures and presence of noise and artifacts in images. To improve segmentation results, deformable models [3] that represent objects in the

form of curves and surfaces can be used. The segmentation process initialized by predefined curves or surfaces consists of transformations that are guided by internal and external forces. The external forces [4, 5] are based on image information and transform surfaces toward object boundaries. The internal forces [6] are defined by curves and surfaces of the model and keep the model connected and smooth. The results can be further improved by using prior knowledge in the form of statistical shape [7] or appearance models [8], estimated from a manually labeled training set. These models represent the segmented object by a predefined number of landmarks, which protect the resulting contour of the model from leakages.

Game theory has been successfully applied to solve multi-criteria optimization problems in the fields of economics, robotics, biology and social sciences. In the field of image analysis, game theory has been applied to calibrate intelligent sensor systems [9] and cameras during surgery [10]. Dynamic programming can be used to solve process management problems by finding the control policy that is based on parameters of the observed process, and has been used to detect curves and boundary segments of objects in images [11]. In this paper we present a segmentation algorithm that identifies landmarks of an anatomical structure by game theory and determines boundary segments between landmarks by dynamic programming. The algorithm was successfully applied to segment lung fields in chest radiographs. However, the algorithm is not limited to these images. It can be used to segment arbitrary objects from two-dimensional (2D) and three-dimensional (3D) images.

2 Landmark detection

This section is organized as follows. Section 2.1 describes a part of game theory named arbitration scheme. Section 2.2 describes landmark detection problem in terms of game theory.

2.1 Arbitration scheme

Game theory is used in a wide range of situations in economy, biology and social sciences, where the success of a decision depends on other decisions. To define a game, a set of “players”, a set of “strategies” that correspond to the players and a set of “incomes” that depend on strategies are required. The game where players can join into a coalition is cooperative, while the game where coalitions between players are not allowed is noncooperative. In a cooperative game, the players can jointly increase their total income and decide how the total income is distributed among them. To

obtain an optimal decision, the Nash arbitration scheme is used which has to satisfy the following conditions [12]:

1) The arbitrage solution is a Pareto-optimal solution. This means that a solution that is better for one player and not worse for the other players does not exist.
2) The arbitrage solution is symmetric. This means that if two players are in the same condition, they must have the same income.
3) The arbitrage solution is invariant to linear transformation.
4) The arbitrage solution is independent of irrelevant alternatives.

An optimal solution $u^* = \left(u_1^*, ..., u_n^*\right)$ is the arbitrage solution of a cooperative game with *n* players:

$$\prod_i \left(u_i^* - d_i\right) = \max_u \prod_i \left(u_i - d_i\right), \tag{1}$$

where $d = \left(d_1, ..., d_n\right)$ is the *status quo* (i.e. incomes of the players if they act individually without joining into coalitions) and $u = \left(u_1, ..., u_n\right)$ is a set of possible incomes that is optimized. Other solutions of a cooperative game exist and can be found by various approaches, e.g. the kernel or Shapley value approach [13, 14]. Since all these techniques are computationally demanding, we used a numerical solution based on the properties of the cooperative game that corresponded to segmentation.

2.2 Landmark detection in terms of game theory

In order to apply game theory to image segmentation, the strategies, players and incomes have to be determined on the basis of image intensities, distinctive anatomical points (i.e. landmarks) and geometrical relationships between them. Suppose that a training set of *N* 2D images with annotated boundaries of objects of interest and landmarks on the boundaries is given in the Cartesian coordinate system (*x, y*). Each landmark is characterized by image intensities in its neighborhood *W* of size $q \times r$ that are normalized by the intensity of the landmark:

$$\bar{W}[x, y] = W[x, y] - I[x_0, y_0], \tag{2}$$

where x_0, y_0 are the landmark coordinates in the training image *I*. A descriptor of a landmark is generated by extracting the neighborhoods of all corresponding landmarks in the training set images and computing the matrices of mean normalized intensity values M_f and standard deviations S_f (Fig. 1). The descriptor is then used to determine candidate points *p* for each landmark in the target image I_a that undergoes the segmentation process. The candidate points correspond to the maxima of the descriptor based similarity measure $\bar{f}$ that evaluates the agreement between the descriptor and image intensities in the neighborhood of each point (x, y) in the image:

$$\bar{f}[x,y] = \sum_{i=0}^{q-1}\sum_{j=0}^{r-1} \frac{1}{S_f[i,j]} e^{-\left(\frac{\left(I_a\left[x+\mathrm{i}-\frac{(q-1)}{2},\,y+\mathrm{j}-\frac{(r-1)}{2}\right]-M_f[i,j]\right)^2}{2S_f[i,j]^2}\right)}. \qquad (3)$$

The descriptor based similarity measure $\bar{f}$ is calculated for each candidate landmark and stored in the matrix $\bar{F}$.

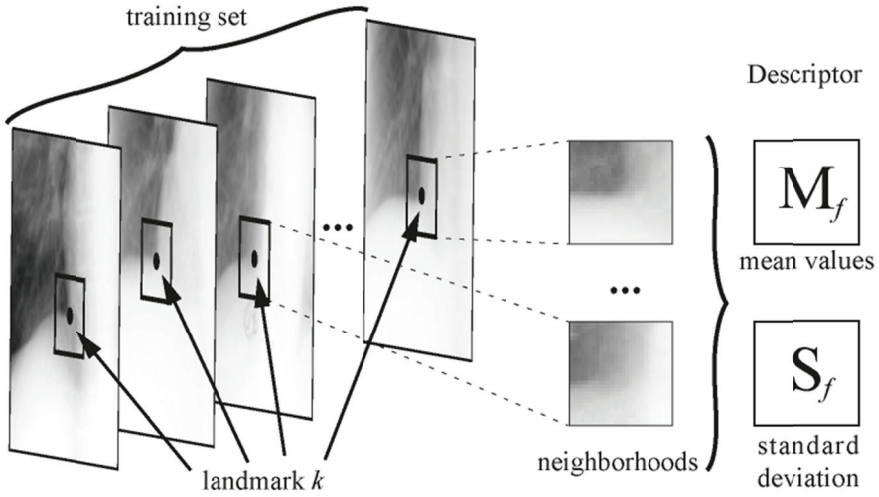

Fig. 1. Generation of the descriptor for landmark *k*. The matrices of mean values M_f and standard deviations S_f are obtained from the normalized neighborhoods.

For each image in the training set, the distance and angle between all pairs of landmarks are also calculated. By averaging the distances over the corresponding pairs of landmarks for all images in the training set, mean distances M_d and standard deviations of distances S_d are obtained. The distance based similarity measure $\bar{d}$

between points p_1 and p_2, which represent candidate points for landmarks l_1 and l_2, respectively, is defined as:

$$\bar{d}(p_1,p_2) = \frac{1}{S_d[l_1,l_2]} e^{-\left(\frac{(d(p_1,p_2)-M_d[l_1,l_2])^2}{2S_d[l_1,l_2]^2}\right)}, \quad (4)$$

where $d(p_1,p_2)$ is the Euclidean distance between points p_1 and p_2 (Fig. 2). The distance based similarity measure $\bar{d}$ is calculated for each ordered pair of landmarks and stored in the matrix $\bar{D}$.

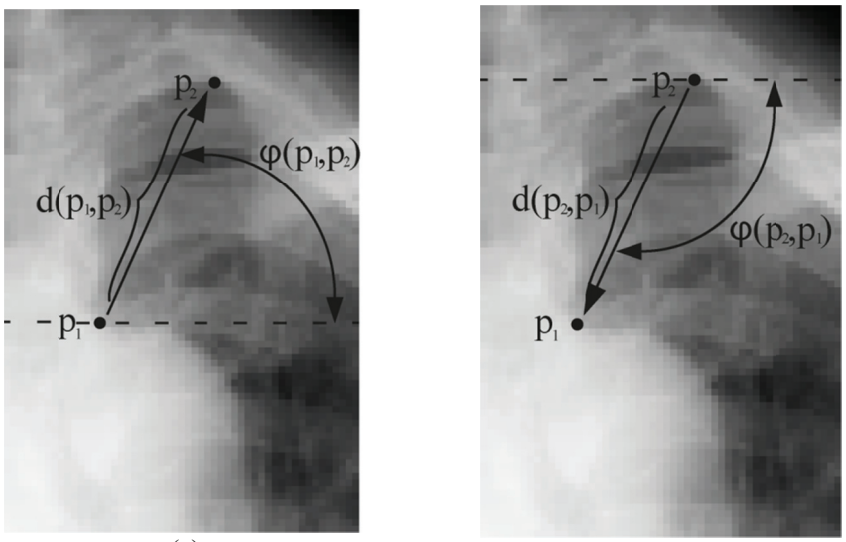

Fig. 2. Example of (a) the distance $d(p_1,p_2)$ and angle $\varphi(p_1,p_2)$ between candidate points p_1 and p_2, and (b) the distance $d(p_2,p_1)$ and angle $\varphi(p_2,p_1)$ between candidate points p_2 and p_1.

By averaging the angles over the corresponding pairs of landmarks for all images in the training set, mean angles M_φ and standard deviations of angles S_φ are obtained. The angle based similarity measure $\bar{\varphi}$ between points p_1 and p_2, which represent candidate points for landmarks l_1 and l_2, respectively, is defined as:

$$\bar{\varphi}(p_1,p_2) = \frac{1}{S_\varphi[l_1,l_2]} e^{-\left(\frac{(\varphi(p_1,p_2)-M_\varphi[l_1,l_2])^2}{2S_\varphi[l_1,l_2]^2}\right)}, \quad (5)$$

where $\varphi(p_1, p_2)$ is the angle of the vector between points p_1 and p_2 in the polar coordinate system (Fig. 2). The angle based similarity measure $\bar{\varphi}$ is calculated for each ordered pair of landmarks and stored in the matrix $\bar{\Phi}$.

With the definition of the descriptor based similarity measure $\bar{f}$ (Eq. 3), distance based similarity measure $\bar{d}$ (Eq. 4) and angle based similarity measure $\bar{\varphi}$ (Eq. 5), the parameters required by the game theory are obtained. The candidate points that are obtained from the descriptor based similarity measure $\bar{f}$ represent the set of strategies, the landmarks represent the set of players, and the distances and angles between landmarks represent the set of incomes. The three-dimensional matrix of incomes *G* is defined as:

$$U[g,i,j] = (1 + \bar{D}[Q[g,0],i,Q[g,1],j] + \bar{\Phi}[Q[g,0],i,Q[g,1],j])\bar{F}[Q[g,0],i], \quad (6)$$

where Q is the set of all ordered pairs of landmarks, g denotes a pair of landmarks (i.e. players l_1 and l_2, then $Q[g,0] = l_1$ and $Q[g,1] = l_2$), i denotes the candidate point for landmark l_1 (i.e. strategy of player l_1), and j denotes the candidate point for landmark l_2 (i.e. strategy of player l_2). The matrix $\bar{F}$ represents the descriptor based similarity measure (Eq. 3) for all landmarks, while matrices $\bar{D}$ and $\bar{\Phi}$ represent the distance and angle based similarity measures (Eqs. 4 and 5), respectively, for all ordered pairs of landmarks (Fig. 3).

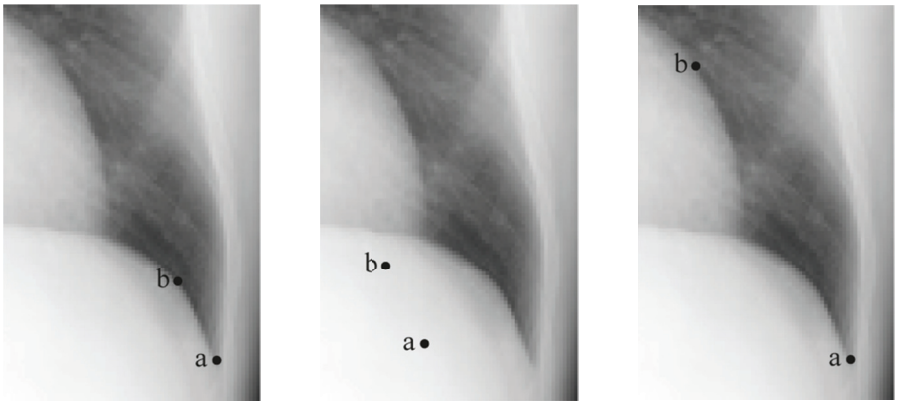

(a) (b) (c)

Fig. 3. (a) The ground truth positions of landmarks *a* and *b*. In this case, the descriptor, distance and angle based similarity are high. (b) The distance and angle based similarity measures are high but the descriptor based similarity measure is low. (c) The descriptor and angle based similarity measures are high but the distance based similarity measure is low.

The cooperative game with the income matrix U has a unique arbitrage solution, which is obtained as the solution that satisfies Eq. 1. The strategies corresponding to the optimal solution are the best positions for the landmarks.

3 Defining of boundary segments

Curves in multi-dimensional spaces can be detected by a dynamic programming that is based on the Bellman principle of optimality. To detect a boundary segment between two adjacent landmarks that is a curve in 2D space, the reagion of the image containing the boundary segment is first approximated by a rectangular strip *T*. This rectangular strip is then filtered by a control matrix *C* to increase the intensity of the boundary segment. The curve that represents the boundary segment is a trajectory that passes through the maximal values of the filtered rectangular strip T_f and is defined from the matrix *R* as the solution of an dynamic programming problem:

$$R[i,j] = T_f[i,j] + \min_{d \in D}(R[i-1, j-d]); \quad T_f = T \times C, \tag{7}$$

where $D = \{-2, -1, 0, +1, +2\}$. To obtain the control matrix *C*, the described procedure (Eq. 7) is iteratively repeated to segment the boundary segment on images from the training set. In each iteration, the matrix *C* is changed and distances between segmented and ground truth boundary segments are measured. By minimizing the measured distances, the matrix *C* is defined. By concatening the trajectories obtained for all adjacent landmarks, the contour of the object is found.

4 Experiments and Results

4.1 Experiments

The proposed segmentation algorithm based on game theory and dynamic programming was successfully applied to segment lung fields from chest radiographs. The chest radiographs and the ground truth segmentation results were obtained from a publicly available database [15, 16] that consists of 247 images of size 256×256 pixels and resolution of 1.4×1.4 mm/pixel. From this database, 82 images (approximately one third of images) were randomly chosen to form the training set. Each image in the training set was manually annotated with 51 approximately equally distributed landmarks on the given lung field contours. The proposed segmentation algorithm was applied to segment the contour of the left and right lung field from the

remaining 165 images in the database. The algorithm was implemented in C++, and the average segmentation time was 11 seconds per image, where the most expensive step was establishing the matrix of incomes (Eq. 6).

4.2 Results

The results were evaluated by an overlap measure Ω between the obtained and ground truth values, which is defined as:

$$\Omega = \frac{TP}{TP + FN + FP}, \tag{8}$$

where the area of the segmented object can be classified as a true positive (TP) (area correctly classified as object), false positive (FP) (area mis-classified as object) or false negative (FN) (area mis-classified as background). Table 1 presents the results of segmentation in terms of overlap and the comparison of the results to segmentation algorithms reported in [16]. An example of the segmentation of lung fields is shown in Figure 4.

Tab. 1. Segmentation in terms of overlap Ω between the obtained and ground truth areas (μ is the mean value, σ is the standard deviation, Q1 is the 0.25-quantile and Q3 is the 0.75-quantile). The results for the existing algorithms were obtained from [16].

	$\mu \pm \sigma$	min	Q1	median	Q3	max
Human observer	0.946 ± 0.018	0.822	0.939	0.949	0.958	0.972
Pixel classification	0.938 ± 0.027	0.823	0.931	0.946	0.955	0.968
Proposed method	**0.916 ± 0.026**	**0.740**	**0.901**	**0.923**	**0.930**	**0.953**
Active shape models	0.903 ± 0.057	0.601	0.887	0.924	0.937	0.960
Active appearance models	0.847 ± 0.095	0.017	0.812	0.874	0.906	0.956

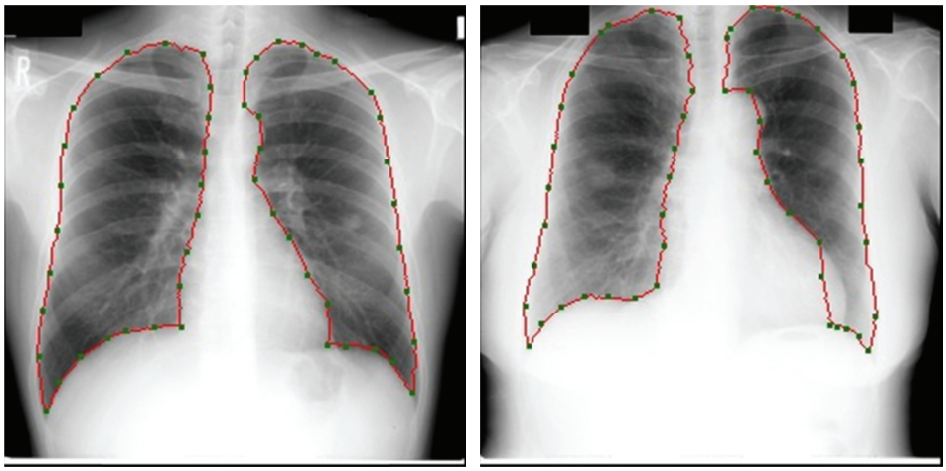

Fig. 4. Examples of detection of landmarks (green squares) and segmentation of lung fields (red lines) in two chest radiographs.

4 Discussion

The proposed algorithm was successfully applied to segment lung fields from 2D chest radiographs. More accurate segmentation results were obtained for the right lung boundary, as the left lung boundary contains parts of the heart and aorta, which introduce large variations of landmark positions (Fig. 4). Moreover, the algorithm can also be used to assist in the initialization of more accurate segmentation methods.

A general disadvantage of the proposed algorithm is the size of the matrix of incomes G (Eq. 6), which amounts to $2n * (n-1) * l * l$, where n is the number of players and l is the number of strategies. While this number is not critical for 2D images, it may result in a lack of available memory of the computer in the case of 3D images. For example, for a 3D image of size 256×256×256 voxels and a description of the object of interest with 200-300 landmarks, the number of elements of the matrix G may exceed 10^9. However, the number of elements can be reduced by using less landmarks (i.e. players) or candidate points for each landmark (i.e. strategies). Taking into account that lung fields are approximately in the middle of a radiograph and not extensively rotated, an area where candidate landmarks are searched for can be reduced. In this way, lower computational times are obtained.

The most important advantage of the algorithm is its wide applicability. The algorithm is independent of translation of the segmented object. If the distance based measure (Eq. 4) is removed from the matrix of incomes (Eq. 6) the algorithm is also independent of scaling of the segmented object. The model introduced by such a

change of the matrix of incomes describes shapes which are independent of the size. Rotation can be eliminated by removing the angle based measure (Eq. 5) from the matrix of incomes (Eq. 6). However, by removing distances or angles from the matrix of incomes (Eq. 6) incorrect segmentations can be obtained.

5 Conclusion

In this paper, a fully automated segmentation algorithm based on game theory and dynamic programming was proposed. The algorithm was applied to lung field radiographs of 247 subjects, and the results show that the performance is comparable with active shape and active appearance models [16].

Acknowledgments

This work has been supported by the Ministry of Higher Education, Science and Technology, Slovenia, under grants P2-0232, J7-2264, L2-7381 and L2-2023.

References

1. Sahoo, P.K., Soltani, S., Wong, A.K.C.: A survey of thresholding techniques. Computer Vision, Graphics, and Image Processing. 41, 233-260 (1988).
2. Gibbs, P., Buckley, D., Blackband, S., Horsman, A.: Tumour volume determination from MR images by morphological segmentation. Physics in Medicine and Biology. 41, 2437-2446 (1996).
3. Caselles, V., Catte, F., Coll, T., Dibos, F.: A geometric model for active contours in image-processing. Numeric Mathematik. 66, 1-31 (1993).
4. Terzopoulos, D., Metaxas, D.: Dynamic 3D models with local and global deformation - deformable superquadrics. IEEE Transactions on Pattern Analysis and Machine Intelligence. 13, 703-714 (1991).
5. Cohen, L.: On active contour models and balloons. CVGIP-Image Understanding. 53, 211-218 (1991).
6. Siddiqi, K., Lauziere, Y., Tannenbaum, A., Zucker, S.: Area and length minimizing flows for shape segmentation. IEEE Transactions on Medical Imaging. 7, 433-443 (1998).
7. Cootes, T., Taylor, C., Cooper, D., Graham, J.: Active shape models - their trainning and application. Computer Vision, Graphics, and Image Processing. 61, 38-59 (1995).
8. Cootes, T., Edwards, G., Taylor, C.: Active appearance models. IEEE Transactions on Pattern Analysis and Machine Intelligence. 23, 681-685 (2001).

9. Bozma, H., Duncan, J.: A game-theoretic approach to integration of modules. IEEE Transactions on Pattern Analysis and Machine Intelligence. 16, 1074-1086 (1994).
10. DeLorenzo, C., Papademetris, X., Staib, L., Vives, K., Spencer, D., Duncan, J.: Image-guided intraoperative cortical deformation recovery using game theory: application to neocortical epilepsy surgery. IEEE Transactions on Medical Imaging. 29, 322-338 (2010).
11. Geinger, D., Gupta, A., Costa, L., Vlontzos, J.: Dynamic-programming for detecting, tracking, and matching deformable contours. IEEE Transactions on Pattern Analysis and Machine Intelligence. 17, 294-302 (1995).
12. Nash, J.: Econometrica. (1950).
13. Raiffa: Contributions to the theory of games, (1953).
14. Shaley, L.: Contributions to the theory of games, (1953).
15. van Ginneken, B.: Image Sciences Institute: SCR database: Result Browser, http://www.isi.uu.nl/Research/Databases/SCR/results/browser.php.
16. van Ginneken, B., Stegmann, M., Loog, M.: Segmentation of anatomical structures in chest radiographs using supervised methods: a comparative study on a public database. Medical Image Analysis. 10, 19-40 (2006).